Monolithically-integrated long vertical cavity surface emitting laser incorporating a concave micromirror on a glass substrate

Rafael I. Aldaz, Michael W. Wiemer, David A.B. Miller, and James S. Harris Jr.

Solid State and Photonics Lab, Stanford University, Stanford, CA 94305
raldaz@snow.stanford.edu

Abstract: We present a fully monolithically integrated long vertical cavity surface emitting laser using an InGaAs/GaAs/AlGaAs gain medium directly bonded to a glass substrate with a concave micromirror. The lasing wavelength is 980nm with a threshold of 20mA for a 52μm mesa, differential quantum efficiency of 58%, and maximum output power of 39mW.

References and links

1. J.G. McInerney, A. Mooradian, A. Lewis, A.V. Shchegrov, E.M. Strzelecka, D. Lee, J.P. Watson, M. Liebman, G.P. Carey, B.D. Cantos, W.R. Hitchens and D. Heald, "High-power surface emitting semiconductor laser with extended vertical compound cavity," Electron. Lett. **39**, 523-525 (2003).
2. D.K. Serkland, P. Esherick, K.M. Geib, G.M. Peake and A.A. Allerman, "Optimization of external cavity VCSELs," in Photonics West, H.Q. Hou, Proc. SPIE **4994**, 30 (2003).
3. E.A. Avrutin, J.H. Marsh and E.L. Portnoi, "Monolithic and multi-GigaHertz mode-locked semiconductor lasers: Construction, experiments, models and applications," IEE Proc., Optoelectron. **147**, 251-278 (2000).
4. P.J. Delfyett, D.H. Hartman and S. Zuber Ahmad, "Optical Clock Distribution Using a Mode-Locked Semiconductor Laser Diode System," J. Lightwave Technol. **9**, 1646-1649 (1991)
5. Ph. Nussbaum, R. Völkel, H.P. Herzig, M. Eisner and S. Haselbeck, "Design, fabrication and testing of Microlens arrays for sensors and Microsystems," Pure Appl. Opt. **6**, 617-636 (1997).
6. H.Y. Wang, R.S. Foote, S.C. Jacobson, J.H. Schneibel and J.M. Ramsey, "Low temperature bonding for microfabrication of chemical analysis devices," Sens. Actuator B-Chem. **45**, 199-207 (1997).
7. L.A. Coldren and S.W. Corzine, *Diode Lasers and Photonic Integrated Circuits* (Wiley Interscience, 1995), Chap. 2.

1. Introduction

Vertical extended cavity surface-emitting lasers (VECSELs) are of general interest because they have most of the advantages of their short cavity counterpart such as wafer level testing, high quality circular beam, and 2D array scalability. But beyond these advantages, the long stable cavity of a VECSEL allows for better transverse mode discrimination, reduced diffraction losses, and high-power high-quality single mode operation. VECSELs may find applications in optical interconnects and amplifiers due to their ability to provide high output powers in a high quality circular beam appropriate for free-space optics and for efficiently coupling into fibers. Such devices have been demonstrated in the past with external mirrors actively aligned to the gain medium [1,2], achieving hundreds of milliwatts of output power while maintaining single transverse mode operation [1]. However, a fully monolithically integrated structure is advantageous to reduce cost and ease mass production.

Vertical long cavity devices are also of interest for mode-locking. These devices are promising sources for wavelength division multiplexing (WDM), optical time division multiplexing (OTDM), optical interconnects, and optical clock distribution [3,4]. Typically, optical filters in the form of partial intracavity mirrors [1,2] are incorporated in the design of

VECSELs to obtain single axial mode operation. However, in the case of mode locking, minimal optical filtering is desired in the cavity to allow the largest possible lasing bandwidth and produce very short high peak power pulses at high repetition rates.
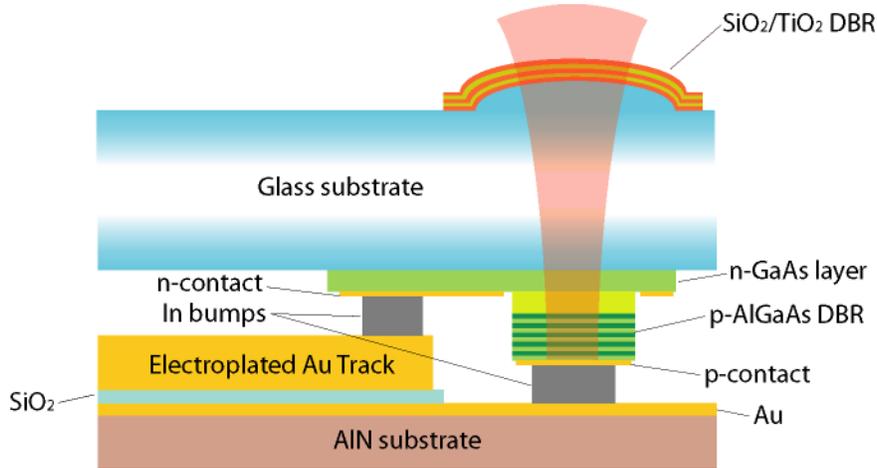

Fig. 1. Schematic of a monolithically integrated vertical long cavity surface emitting laser.

In this work we demonstrate a fully monolithically integrated vertical long cavity surface emitting laser using a glass substrate as the cavity. Figure 1 shows the general schematic of the device. A stable laser cavity is formed between an AlGaAs/GaAs Distributed Bragg Reflector (DBR) and a concave mirror on the glass substrate serving as the output coupler. The gain medium is located in between the DBR and the glass substrate and is electrically pumped through an intracavity contact and the semiconductor DBR. The laser sits on a heatsink for electrical contact and proper heat dissipation. The cavity has minimal optical filtering designed to obtain broad lasing bandwidth.

2. Resonator design

In general, a flat-concave mirror resonator has to have R > L to be stable, where R is the radius of curvature (ROC) of the concave mirror and L is the total length of the resonator. The electric field spot diameters for a fundamental gaussian beam will be given by:

$$2\omega_{flat} = 2\sqrt{\frac{\lambda}{n\pi}\sqrt{LR - L^2}} \tag{1}$$

$$2\omega_{concave} = 2\sqrt{\frac{\lambda}{n\pi}\sqrt{\frac{L^2R^2}{LR - L^2}}} \tag{2}$$

Where λ is the wavelength, n is the index of refraction of the medium, and ω is the radius of the gaussian beam. At the location of the concave mirror, the resonant beam will have a wavefront curvature equal to that of the mirror. Therefore, the beam will be perpendicularly incident upon the curved DBR stack at every point, requiring no further engineering of the layers in the stack.

A small gain mesa size is desired to lower the threshold currents and improve device efficiency. However, the mesa should be large enough to keep the aperture loss below an upper limit and account for fabrication misalignment between the two mirrors. For this first attempt, we have chosen mesa diameters of 3 times the electric field spot diameter plus 10μm for misalignment tolerances.

3. Fabrication

Microlens arrays were fabricated on a 500μm thick fused quartz wafer by photoresist reflow and dry-etching shape transfer techniques [5]. Smooth microlenses were obtained with rms roughness of the order of 10Å measured by AFM. The 99% reflecting concave micromirrors were formed by depositing a SiO_2/TiO_2 DBR on the microlenses. After dicing, each array was bonded at room temperature [6] to a similar size piece of active epitaxial material. The epitaxial structure consisted of a p-doped highly reflective 32-pair AlGaAs DBR followed by 3 sets of 3 $In_{0.14}Ga_{0.86}As$ MQWs surrounded by GaAsP strain compensating barriers and a n-doped contacting layer. The structure was grown up-side down with an $Al_{0.95}Ga_{0.05}As$ release layer in between the GaAs substrate and the AlGaAs DBR.

After bonding, the GaAs substrate and release layer were selectively etched away leaving a very thin layer of semiconductor material on the glass substrate. Photoresist mesas were lithographically defined on the semiconductor layer and aligned to the micromirror array on the backside of the glass substrate. The mesas were etched down to the n-contact layer by reactive ion etching (RIE). A second mesa was also etched to isolate the n-contact layer of each device. Finally, n- and p-type metal contacts were deposited and annealed.

Processing temperature is one of the major issues when fabricating these devices because of the stress caused by the different thermal expansion coefficients between materials. Each step had to be carefully designed to avoid the GaAs epitaxy and glass from debonding or the DBR stack on the curved micromirrors from cracking.

The heatsinks were fabricated on both AlN and Si substrates. A first metal contact layer was deposited on the substrate followed by an isolating SiO_2 layer. A second metal contact layer was then deposited on top of the SiO_2 to serve as a seed layer during electroplating. After lithographically defining the openings for the tracks, the sample was electroplated to achieve a thickness equal to the height difference between the p- and n-contact layers of the active region of the laser. Next, the photoresist was removed, the seed layer was etched away to isolate the tracks, and the isolating SiO_2 layer was dry-etched to expose the first contacting layer. Indium bumps were deposited on top of the tracks and bottom contact layer to finally flip-chip bond the laser arrays to the heatsink.

This fabrication process is also valid for integrating other semiconductor gain materials at different wavelengths.

4. Device results

A silicon heatsink with an array of devices was placed on a cooled copper chuck for testing. The devices were tested CW at a chuck temperature of 15°C, corresponding to a device temperature at the indium bond of approximately 36°C at 90mA pump current [7]. Figure 2(a) shows the output power and voltage drop vs. input current for a 52μm mesa device with a 167μm diameter micromirror and 600μm ROC. For comparison, the electric field spot diameters of the fundamental transverse mode for this configuration are 14μm at the flat mirror and 34μm at the curved mirror according to Eq. (1) and Eq. (2). The threshold current was 20mA with a differential quantum efficiency of 58%. The maximum power obtained out of this device was 39mW before rolling-over. The output transverse mode remained stable during operation, however the shape resembled that of a higher order mode. It is believed single transverse mode operation can be achieved by further confining the current injection to obtain a more uniform gain profile and better overlap with the fundamental optical mode. Higher output powers should be achievable by optimizing the output coupler with respect to the device total gain and loss, improving the overlap of the gain and optical mode thus increasing efficiency, and engineering better heatsinks to push the roll-over point to higher injection currents.

The spectrum of the laser for three injected currents is shown in Fig. 2(b). The broad lasing bandwidth is approximately 3nm wide and red-shifts as the current injection increases. The main peaks of the spectrum at 90mA are spaced by approximately 0.65nm or 200GHz,

which corresponds to the axial mode spacing expected from a 500μm thick glass cavity. The sidebands surrounding each main peak indicate the presence of higher order transverse modes.
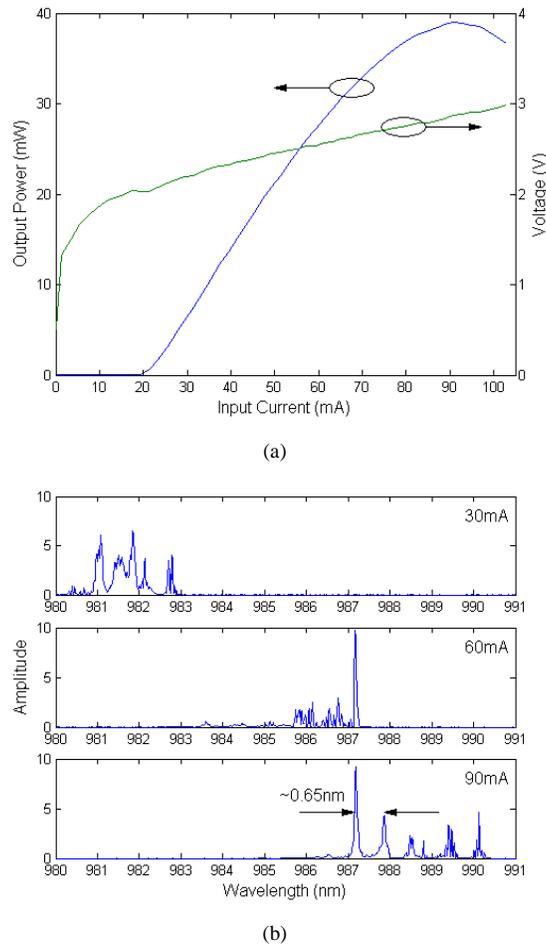

(a)

(b)

Fig. 2. (a) Output power and voltage drop vs. input current for a device with a 52μm mesa and a 600μm ROC micromirror. (b) Lasing spectrum of the same device for three input currents.

As opposed to conventional vertical-cavity surface-emitting lasers (VCSELs) or VECSELs, we believe the roll-over and spectrum shift mechanism of our device is not due to the poor overlap of the cavity mode with the gain peak or simple cavity mode shift. In conventional VECSELs, the single axial mode is strongly defined by the finesse of the gain cavity. As the temperature in the cavity increases, the gain peak wavelength red-shifts faster than the cavity mode, decreasing the overlap between the two and therefore causing the output power to drop. In our device, there is not a very strong resonance in between the semiconductor DBR and the GaAs/glass interface. Therefore, multiple closely spaced axial modes, mainly defined by the length of the glass substrate, could lase under the gain peak. As the temperature increases, the gain peak red-shifts causing new axial modes to lase, as shown in Fig. 2(b). Instead, it is the spatial overlap of the standing wave of the new axial modes with the MQWs that decreases as the gain peak shifts, causing the output power to roll-over.

5. Conclusions

We have presented a fully monolithically integrated long vertical cavity surface emitting laser using a glass substrate as the cavity and incorporating a concave micromirror. We have demonstrated CW operation at 980nm with threshold currents of 20mA for a 52μm mesa with 58% differential quantum efficiency and 39mW maximum output power. The device showed the broad lasing bandwidth necessary for producing high-power short-pulses when mode-locked. This structure is a promising way of achieving the performance of a VECSEL with the fabrication advantages of a VCSEL.